JOURNAL OF MATERIALS SCIENCE: MATERIALS IN MEDICINE 6 (1995) 206–210

XRD and XPS characterization of superplastic TiO_2 coatings prepared on Ti6Al4V surgical alloy by an electrochemical method

M. SHIRKHANZADEH
Department of Materials & Metallurgical Engineering Queen's University, Kingston, Ontario, K7L 3N6 Canada

X-ray diffraction (XRD) and X-Ray photoelectron spectroscopy (XPS), in conjunction with argon ion etching, were used to characterize the microstructure and the chemical composition of alkoxy-derived TiO_2 coatings prepared on Ti6Al4V surgical alloy by an electrochemical method. The as-deposited oxide coatings prepared at room temperature (up to 40 μm thick) were amorphous, but transformed into nanocrystalline anatase at 550 °C. Using a micro-indentation technique, it was found that nanocrystalline anatase coatings were ductile, permitting significant plastic deformation at room temperature. The XPS data also revealed the presence of significant proportion of physisorbed (OH) and chemisorbed H_2O (i.e. Ti–OH) on the oxide surface, indicating that these coatings, similar to sol–gel-prepared titania, may serve as reactive substrates for heterogeneous nucleation of apatite under physiological conditions.

1. Introduction

It is now recognized that direct bonding between bone and the surface of a load-bearing implant is essential for its long-term clinical success. Several materials, including commercially pure titanium [1], are capable of forming direct bond with bone. In the case of titanium, light microscopic and ultrastructural analysis have revealed evidence of osseointegration, a direct bone-to implant contact [2]. The excellent tissue response to titanium is believed to be related to the chemical and biochemical properties of titanium oxide at the titanium surface [3]. Ducheyne *et al.* have studied changes in titanium oxide composition as a function of exposure to human serum [4]. It was reported that after extended exposure, the surface concentration of OH groups increased significantly and Ca and P were substituted for the hydrated oxide. Tengwall *et al* [5] have also proposed than an interaction between the surface oxide and hydrogen peroxide released from the biological process could leave a titanium peroxy gel with abundant OH groups on the titanium implant, which seems to be responsible for biocompatibility of titanium. Pretreatment of titanium implants with hydrogen peroxide has been suggested to accelerate the process leading to osseointegration [6]. More recently, Li *et al.* [7] have demonstrated that hydrated alkoxy-derived anatase films fabricated by sol–gel method can effectively induce formation of bone-like hydroxyapatite when incubated in metastable calcium phosphate solutions.

We have recently reported a novel electrochemical method for preparing alkoxy-derived titanium oxide coatings (up to 40 μm thick) at room temperature [8, 9]. Previous work [9] has indicated that alkoxy-derived coatings prepared by the electrochemical method can effectively minimize the rate of metal-ion release from Ti6Al4V surgical alloy. It was also demonstrated that such coatings can act as effective substrates for electrocrystallization of apatite from aqueous solutions [10]. More recent work [11] has shown that alkoxy-derived oxide coatings obtained by this process exhibit superplasticity at room temperature.

The aim of the present study is to further characterize the microstructure and the chemical composition of alkoxy-derived TiO_2 coatings and evaluate their potential use as bone-bonding interfaces for load-bearing implants.

2. Materials and methods

The coating process for the electrochemical fabrication of alkoxy-derived TiO_2 coatings has been described previously [9]. The process involves direct synthesis of titanium methoxide ($Ti(OCH_3)_4$) by anodic oxidation of titanium in methanolic electrolytes and its rapid hydrolysis and conversion into titanium oxide in the presence of water. Rectangular samples of Ti6Al4V surgical alloy (5 × 1 cm) were mechanically polished and used as the substrate (anode). The electrolyte used was prepared by adding 10 g of analytical reagent sodium nitrate ($NaNO_3$) to 1 *l* of analytical reagent methanol containing less than 1% water. TiO_2 coatings up to 40 μm thick were obtained at room temperature using constant current densities ranging from 5 to 20 mA/cm^2.

0957–4530

X-ray photoemission spectroscopy (XPS) and argon ion etching were employed to identify the surface molecular species and chemical composition of the oxide coating at depth. Analysis was done using a modified spectrometer equipped with a monochromatized AlK_α X-ray small spot probe. Survey spectra were obtained with 600 μm spot size and a 150 eV pass energy. Sputtering was carried out with 4 kV argon ions with an approximate sputter rate of 10 nm/min for SiO_2. The microstructure of the oxide coating was also determined by scanning electron microscopy (SEM) and X-ray powder diffraction (XRD) techniques. In addition, the low temperature ductility of the coatings was evaluated by indentation and microhardness measurement at room temperature.

3. Results and discussion

3.1. SEM and X-ray diffraction analysis

Fig. 1 shows an SEM micrograph of the cross-section of a typical titanium oxide coating on Ti6Al4V substrate. The oxide coatings as prepared at room temperature were dense, uniform and well adhered to the substrate. In Figs 2 and 3, XRD patterns are shown for the titanium oxide powder removed from the substrate. Diffraction patterns were obtained for the oxide powder without heat treatment and after heat treatment at temperatures ranging from 100 to 800 °C for 30 min. X-ray patterns were analysed over a range of 2θ values between 20° and 34°, as this contains major peaks corresponding to anatase and rutile. The as-deposited coatings were amorphus, but crystallized to anatase at 550 °C. A significant orientation along the [1 0 1] direction was observed for crystalline anatase coatings. The average crystallite size of the anatase coating heat treated at 550 °C was estimated from the line broadening of the [1 0 1] peak at half the maximum intensity, using the Scherrer formula [12]. The average crystallite size was 3 nm. It should be noted, however, that absolute accuracy in the line-broadening X-ray diffraction technique is about 25% in this size range [13]. The X-ray patterns

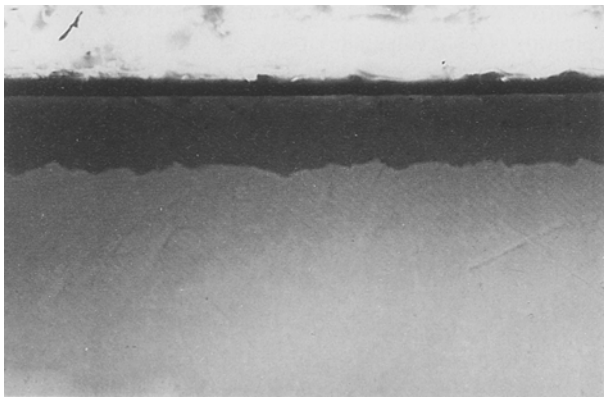

Figure 1 SEM micrograph of a typical amorphous anatase coating prepared on a polished Ti6Al4V substrate at 7 mA cm^{-2} for 1 h at 25 °C (X800).

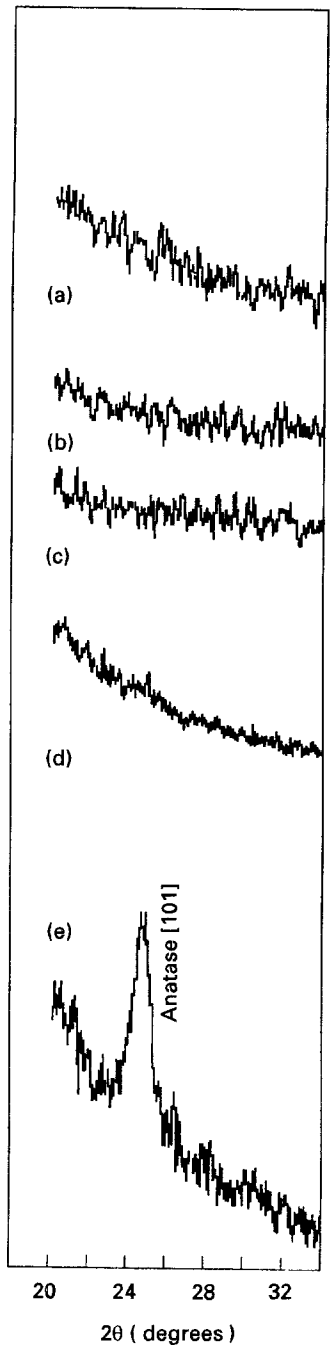

Figure 2 X-ray diffraction pattern of (a) untreated oxide, and heat-treated oxide at (b) 100 °C, (c) 300 °C, (d) 500 °C, and (e) 550 °C for 30 min.

in Figs 2 and 3 indicate an increase in crystal size of the coating with increased heat treatment temperature. The anatase-to-rutile transformation temperature was found to be about 700 °C, but complete transformation of anatase to rutile was not observed even at 800 °C. Complete transformation, however, would be expected for samples heat treated at higher temperatures and for relatively longer periods.

Nanocrystalline anatase coatings are expected to exhibit superplasticity at room temperature. In the present work, the room temperature ductility of nanocrystalline anatase coating was investigated by measuring its Vickers hardness. Hardness was determined, using a 3N indent made with a Vickers diamond indentor at room temperature. Vickers hardness of the nanocrystalline coating was compared with

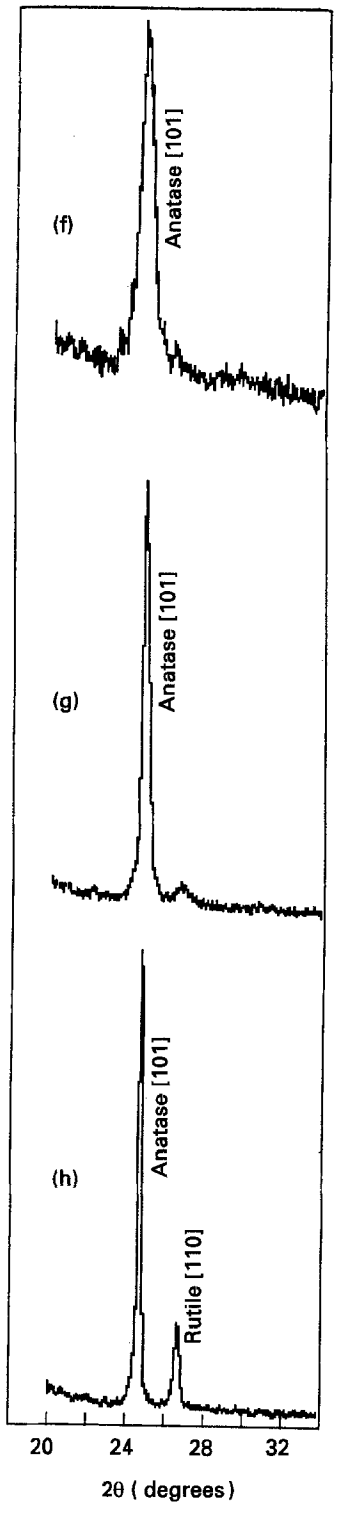

Figure 3 X-ray diffraction patterns of the oxide heat-treated at (f) 600 °C, (g) 700 °C, and (h) 800 °C for 30 min.

that of polycrystalline titania ($H_V \approx 800$ [14]). The hardness of the nanocrystalline coating measured was 280 H_V (less than half of that of polycrystalline titania). A relatively low Vickers hardness was also reported by Karch *et al.* for nanocrystalline TiO_2 obtained by gas condensation technique [14]. The low Vickers hardness of the nanocrystalline TiO_2 was interpreted in terms of its enhanced diffusional creep and superplasticity at room temperature. Fig. 4 shows the plastic deformation of the nanocrystalline anatase coating by indenting at room temperature. Indentation of conventional polycrystalline titania under similar condition has shown to result in multiple cracking [14]. These results indicate that alkoxy-derived anatase coatings prepared by electrochemical method may exhibit superplasticity at body temperature and may be potentially useful coatings for load-bearing implants.

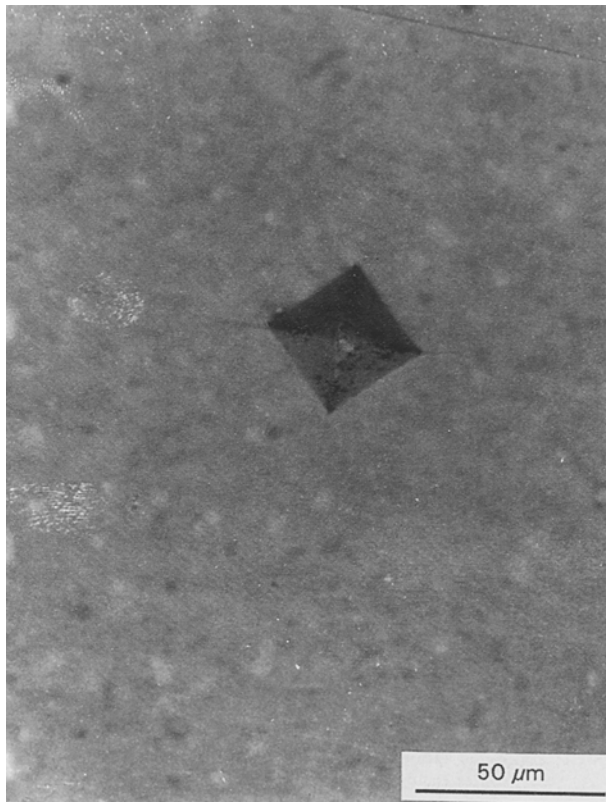

Figure 4 Plastic deformation of nanocrystalline anatase coating by indenting at room temperature (load 3N deformation time 30 s).

3.2. X-ray photoelectron spectroscopic characterization of the oxide coatings

Fig. 5 shows a typical XPS survey spectrum from the surface of anatase coating on a Ti6Al4V specimen. The dominant signals are Ti, O, and C, with weaker contribution from N and Al. These observations were also confirmed by Auger electron spectroscopy analysis [9]. High resolution spectra of the Ti_2p peak (Fig. 6) shows that the surface oxide consists mainly of titanium (IV) oxide. The peak at 458.5 eV was attributed to $Ti^{4+}2p_{3/2}$ and the peak at 464.2 eV to $Ti^{4+}2p_{1/2}$. The results indicate that suboxides such as TiO, Ti_2O_3 and Ti_3O_5 are not present on the oxide surface. Further information on the chemical composition of the oxide surface comes from high resolution XPS O1s spectra (Fig. 7). Gopel *et al.* [15] have shown that the O1s spectra for titanium (IV) oxide is symmetric. The results in Fig. 7 shows an asymmetrical broadening toward the higher binding energy side of the major peak, indicating the presence of other species on the surface. To identify these species, Gaussian model peaks were fitted to the spectra in Fig. 7. The major peak at 530.4 eV was attributed to bulk oxygen of TiO_2 [15] and the subpeaks at 531.9 and

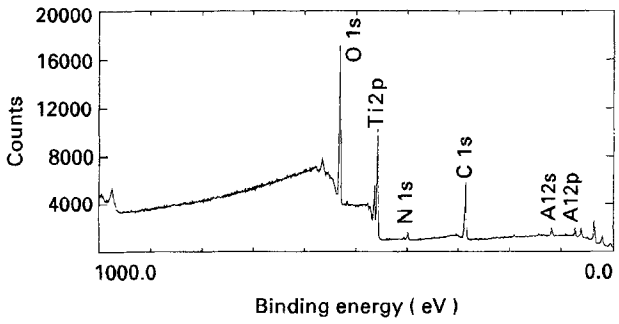

Figure 5 XPS survey spectrum of nanocrystalline anatase coating before Ar^+ ion sputtering.

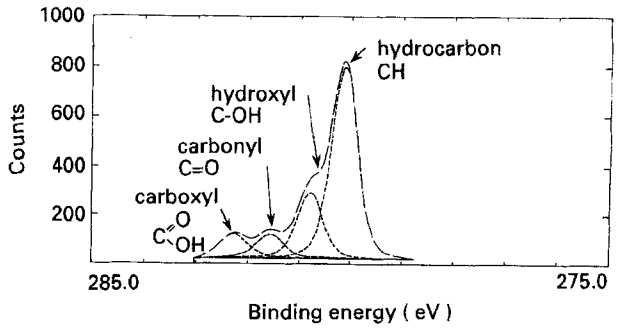

Figure 8 High resolution XPS spectrum of the C 1s peak at the oxide surface.

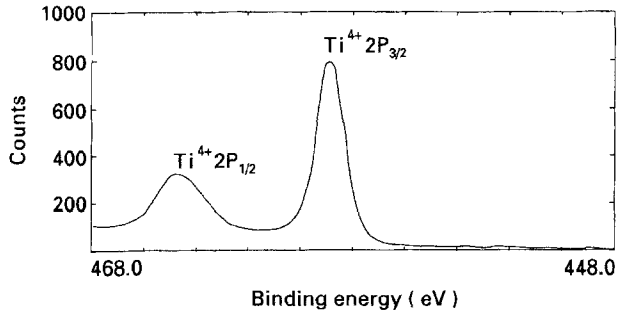

Figure 6 High resolution XPS spectrum of the Ti2p peak at the oxide surface.

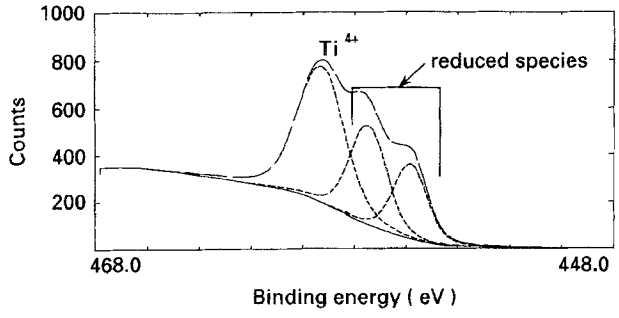

Figure 9 High resolution XPS spectrum of the Ti2p peak after Ar^+ ions sputtering for 2 min.

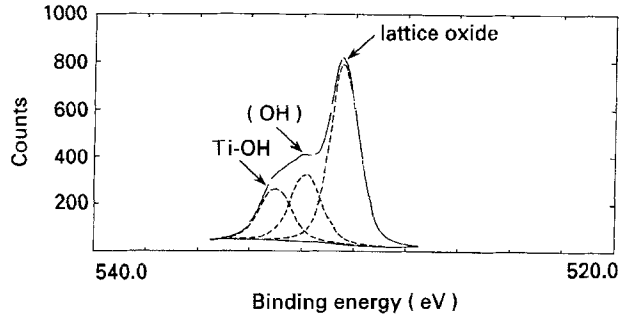

Figure 7 High resolution XPS spectrum of the O 1s peak at the oxide surface.

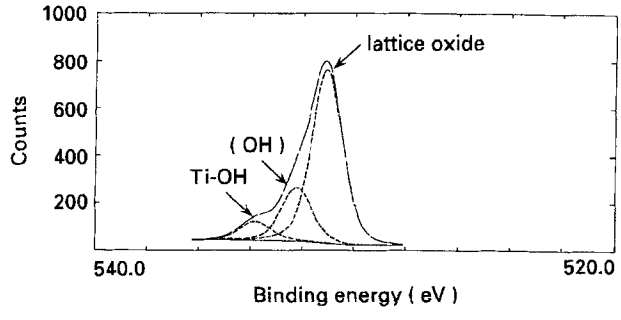

Figure 10 High resolution XPS spectrum of the O 1s peak after Ar^+ ion sputtering for 2 min.

533 eV were attributed to physisorption of (OH) and chemisorbed H_2O (i.e. TiOH), respectively.

The asymmetrical broadening of the major peak in the C1s spectrum in Fig. 8 also indicates that multiple C species are present on the oxide surface. Curve fitting of C1s lines exhibits four components which correspond to hydrocarbon or graphite (285.2 eV), C–OH (286.5 eV), C = O (289.1 eV) and $\overset{O}{\overset{\|}{C}}$–OH (289.5 eV) [16]. After sputtering with Ar^+ ions for 2 min, carbon signals were significantly reduced, indicating that C species were mainly located on the oxide surface.

Fig. 9 shows high resolution XPS Ti2p spectra taken at depth after sputtering for 2 min. The Ti2p spectra shows that there is a contribution from titanium with lowered valency state in the coating, indicating that at depth, the coating stoichiometry is disturbed and TiO_2 tends towards suboxide states. This observation may be partly associated with the sensitivity of Ti (IV) ions towards the bombardment with Ar^+ ions. The formation of titanium suboxides upon argon ion etching is consistent with the behaviour observed by other researchers [17].

The high resolution O1s spectra after 2 min sputtering (Fig. 10) showed contribution of (OH) groups at depth in the coating, indicating that these species were not exclusively located on the surface. It is speculated that during the coating process, an inorganic network consisting of Ti–O–Ti bridges is initially formed as a result of hydrolysis and controlled polycondensation of titanium methoxide. The terminating bonds of this oxide polymer contains (OH) and probably (OR) groups. It is known that the polycondensed materials from metal alkoxides can never be 100% oxide since this would require an infinite polymer with no terminal bonds [18]. It is interesting to note that the asymmetric broadening associated with the surface hydroxyl groups in O1s spectra (Fig. 7) contributes

significantly to the total core level intensity. Thus, it is envisaged that numerous hydroxyl groups may remain on the oxide surface. It is known that anatase could be charged negatively in physiological solutions (pH = 7.4), since the point of zero charge (PZC) of this oxide is pH 6.2 [19]. Calcium ions may therefore, be attracted to anatase surface under physiological conditions. On the other hand, the hydroxyl groups on the anatase surface may facilitate bonding of phosphate groups through a hydrogen bond [20]. The formation of apatite on the anatase surface can be initiated once the supersaturation exceeds the level necessary for heterogenous nucleation [7]. Nucleation and crystallization of Ca-deficient apatite on cathodically charged anatase coatings has indeed been demonstrated [8, 10]. These results suggest that alkoxy-derived anatase coatings prepared by electrochemical method, similar to gel-derived titania [7], may serve as reactive substrates for nucleation and growth of apatite under physiological conditions. It is also proposed that cathodic charging of anatase coatings in electrolytes containing Ca- and P-bearing ions [10], may further enhance bioactivity of these coatings *in vivo*, and may accelerate the process leading to osseointegration.

4. Conclusions

The X-ray and XPS results have shown that alkoxy-derived anatase coatings prepared by an electrochemical method have interesting microstructure and surface properties. Based on XRD and XPS data, these coatings are expected to exhibit superplasticity at low temperatures and may act as reactive substrates for heterogeneous nucleation of apatite under physiological conditions.

Acknowledgement

The author thanks the Natural Sciences and Engineering Research Council of Canada (NSERC) for the financial support provided for this research project.

References

1. Z. SCHWARTZ, D. AMIR, B. D. BOYAN, D. KOHAVL, C. MULLER MAI, L. D. SWAIN, U. GROSS and J. SELA, *Calcif. Tissue. Int.* **49** (1990) 1.
2. C. JOHANSSON, T. ALBREKTSSON, *J. Oral Maxillofac. Implants* **2** (1987) 69.
3. B. KASEMO, *J. Prosthet. Dent.* **49** (1989) 832.
4. K. E. HEALY and P. DUCHEYNE, *Biomaterials* **13** (1992) 553.
5. P. TENGWALL and I. LUNDSTROM, *Clin. Mater.* **9** (1992) 115.
6. P. TENGWALL, I. LUNDSTROM, L. SJOKVIST, H. ELWING, and L. M. BJURSTEN, *Biomaterials* **10** (1989) 166.
7. P. LI and K. DE GROOT, *J. Biomed. Mater. Res.* **27** (1993) 1495.
8. M. SHIRKHANZADEH, US patent 5,211,833 (1993).
9. *Idem., J. Mater. Sci. Mater. Med.* **3** (1992) 322.
10. *Idem., Mater. Lett.* **14** (1992) 27.
11. *Idem., ibid.*, **16** (1993) 189.
12. H. P. KLUG and L. E. ALEXANDER, "X-ray diffraction procedures" (Wiley, New York, 1970).
13. R. C. GRAVIE, *J. Phys. Chem.* **69** (1965) 1238.
14. J. KARCH, R. BIRRINGER and H. GLEITER, *Nature* **330** (1987) 556.
15. W. GOPEL, J. A. ANDERSON, D. FRANKEL, M. JAEHNIG, K. PHILLIPS, J. A. SCHAFER and G. ROCKER, *Surf. Sci.* **139** (1984) 333.
16. D. T. CLARK and H. R. THOMAS, *J. Polym. Sci. Polym. Chem. Ed.* **16** (1978) 791.
17. S. M. ROSSNAGEL and J. R. SITES, *J. Vac. Sci. Technol.* **2** (1984) 376.
18. B. E. YOLDAS, *J. Mater. Sci.* **10** (1986) 1087.
19. G. A. PARKS, *Chem. Rev.* **65** (1965) 177.
20. D. E. C. CARBRIDGE, "The structural chemistry of phosphorus" (Elsevier, Amsterdam, 1974).

Received 31 January
and accepted 29 June 1994